Journal Pre-proof

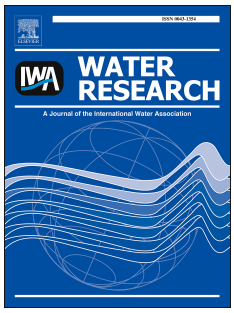

Dissolved organic matter in a tropical saline-alkaline lake of the East African Rift Valley.

A. Butturini, P. Herzsprung, J. Lechtenfeld O, S. Venturi, S. Amalfitano, Vazquez E, N. Pacini, D.M. Harper, F. Tassi, S. Fazi

PII: S0043-1354(20)30068-3

DOI: https://doi.org/10.1016/j.watres.2020.115532

Reference: WR 115532

To appear in: *Water Research*

Received Date: 20 June 2019

Revised Date: 10 December 2019

Accepted Date: 20 January 2020

Please cite this article as: Butturini, A., Herzsprung, P., Lechtenfeld O, J., Venturi, S., Amalfitano, S., E, V., Pacini, N., Harper, D.M., Tassi, F., Fazi, S., Dissolved organic matter in a tropical saline-alkaline lake of the East African Rift Valley., *Water Research* (2020), doi: https://doi.org/10.1016/j.watres.2020.115532.

Dissolved organic matter in a tropical saline-alkaline lake of the East African Rift Valley.

Authors and affiliations

Butturini A.[a*], Herzsprung P.[b], Lechtenfeld O. J.[c], Venturi S.[g, h], Amalfitano S.[d], Vazquez E., Pacini N.[f], Harper D.M.[e], Tassi F.[g,h], Fazi S.[d].

[a] Department de Biologia evolutiva, Ecologia y Ciencies ambientals, Universitat de Barcelona, Catalonia, Spain.

[b] Department Lake research, Helmholtz Centre for Environmental Research, Magdeburg, Germany.

[c] Department Analytical Chemistry, Research group BioGeoOmics, Helmholtz Centre for Environmental Research, Leipzig, Germany.

[d] CNR – IRSA Water Research Institute, Via Salaria km 29.300 – CP10, 00015 Monterotondo, Rome, Italy.

[e] Aquatic Ecosystem Services, Ltd., Drabblegate, Aylsham, Norfolk, United Kingdom.

[f] Department of Environmental and Chemical Engineering, University of Calabria, Rende, Cosenza, Italy.

[g] Department of Earth Sciences, University of Florence, Via G. La Pira 4, 50121 Florence, Italy.

[h] CNR – IGG Institute of Geosciences and Earth Resources, Via G. La Pira 4, 50121 Florence, Italy.

*Corresponding author: abutturini@ub.edu

Abstract

Saline-alkaline lakes of the East African Rift are known to have an extremely high primary production supporting a potent carbon cycle. To date, a full description of carbon pools in these lakes is still missing. More specifically, there is not detailed information on the quality of dissolved organic matter (DOM), the main carbon energy source for heterotrophs prokaryotes. We report the first exhaustive description of DOM molecular properties in the water column of a meromictic saline-alkaline lake of the East African Rift. DOM availability, fate and origin were studied either quantitatively, in terms of dissolved organic carbon (DOC) and nitrogen (DON) or qualitatively, in terms of optical properties (absorbance) and molecular characterization of solid-phase extracted DOM (SPE-DOM) through negative electrospray ionization Fourier Transform Ion Cyclotron Resonance Mass Spectrometry (FT-ICR-MS). DOM availability was high (DOC ~ 8.1 mM in surface waters) and meromixis imprinted a severe quantitative and qualitative change on DOM pool. At the surface, DOM was rich in aliphatic and moderately in aromatic molecules and thus mirroring autochthonous microbial production together to photodegradation. At the bottom changes were extreme: DOC increased up to 5 times (up to 50 mM) and, molecular signature drifted to saturated, reduced and non-aromatic DOM suggesting intense microbial activity within organic sediments. At the chemocline, DOC was retained indicating that this interface is a highly reactive layer in terms of DOM processing. These findings underline that saline-alkaline lakes of the East African Rift are carbon processing hot spots and their investigation may broaden our understanding of carbon cycling in inland waters at large.

Key words: Dissolved organic carbon, African soda lake, Meromixis, FT-ICR-MS, CDOM

1. Introduction

Endorheic saline-alkaline lakes are known from all continents. In terms of water volume and surface, they represent 40% and 20% of total lakes, respectively (Meybeck, 1995; Dodds and Whiles, 2002; Wurtsbaugh et al., 2017). The saline-alkaline lakes of the East African Rift (thereafter SLARs) are among the most distinctive in the world. SLARs contribute up to ~75% of total lake area in this region and cover a total area of ~13000 km^2 with single lake areas ranging from 8800 km^2 (Lake Turkana) down to tens of crater lakes smaller than 0.5 km^2.

Their pH and alkalinity are typically in excess of 9.5 and 50 meq L^{-1}, respectively (Hecky and Kilham, 1973). A striking feature is a daily pelagic primary production of over than 10 g O_2 m^{-2} (Melack, 1982; Oduor and Schagerl, 2007), which is significantly higher than that recorded in freshwater ecosystems (Lewis, 2011). This high productivity is sustained by planktonic cyanobacteria (up to 10^7-10^8 cells ml^{-1}, Zinabu and Taylor, 1997) that proliferate owing to constant high water temperatures (> 20 ^oC, the "endless summer" according to Kilham and Kilham, 1989), intense and almost constant solar radiation throughout the year at Equator (~173 W m^{-2}; Odongo et al., 2016), and very high availability of dissolved inorganic carbon (Talling et al., 1973).

Overall, SLARs showed a very dynamic carbon cycle, yet a clear picture of carbon availability and fluxes is still lacking. In particular, information about dissolved organic matter (DOM) and its qualitative properties is largely disregarded and incompletely understood (Jirsa et al., 2013). DOM is a complex mixture of highly diverse molecules that differ in composition, structure, origin, residence time and bioavailability (Dittmar and Stubbins, 2014). Besides being the indispensable source of carbon and energy for the aquatic microbiota, DOM interacts with light by attenuating and modifying the underwater radiation spectra (Thrane et al., 2014) and is adsorbed to minerals or desorbed after reductive dissolution of iron minerals (Elkins and Nelson, 2002).

The objective of this study is to provide a first exhaustive description of the DOM quantity and molecular properties in a SLAR. Having in mind that, at the Equator, the seasonal changes are reduced (Odongo et al., 2016), this study specifically focused on a meromictic lake with severe biogeochemical gradients along the water column (Melack, Kilham and Fisher, 1982; MacIntyre and Melack, 1982). In particular we aimed to provide a better understanding of the impact of (i) water stratification, (ii) pelagic primary production and photodegradation. DOM was analyzed to (a) quantify it in terms of dissolved organic carbon (DOC) and nitrogen (DON) (b) describe its spectroscopic properties through absorbance, and (c) characterize its molecular property through Fourier Transform- Ion Cyclotron Resonance Mass Spectroscopy (FT-ICR-MS).

High primary production together with high potential evaporation is expected to determine large DOC concentrations in the water column. High density of pelagic cyanobacteria and high and constant incident solar radiation are likely to strongly affect DOM quality as well. Cyanobacteria release aliphatic compounds (Bittar et al., 2015) as a consequence, saturated (H/C>1.5) and relative oxygen-poor (O/C<0.5) molecules might be significant. Simultaneously, aromatic compounds are expected to be low as consequence of photodegradation induced by elevated incident radiation.

2. Material and methods

2.1. Study site and sampling strategy

Lake Sonachi (90 km NW of Nairobi at 1,884 m a.s.l.; 0°46'57.68"S; 36°16"E) is a small (0.18 km^2) meromictic saline-alkaline lake located in a volcanic crater (0.84 km^2) surrounded by riparian vegetation (mainly *Vachellia xanthophloea*) (MacIntyre and Melack, 1982) and adjacent to the larger freshwater Lake Naivasha (c.a. 150 km^2) (Figure SI 1). Climate is warm

and semiarid, with annual potential evaporation (ca. 1800 mm/year Olaka, 2011) exceeding annual precipitation (ca. 640 mm/year www.climatedata.eu).

Groundwater seepage from Naivasha is likely to be the main water input, whereas evaporation is the outflow (Gaudet and Melack, 1981). A steep crater rim protects the lake from winds and the water column mixing is limited (MacIntyre and Melack, 1982).

Water column depth varied from 3 m to 18 m with generally stable meromictic conditions. Holomixis episodes were reported only during low water level periods (MacIntyre and Melack, 1982; Verschuren, 1999). Primary production ranged from 2.2 to 56 mM O_2 m^{-3} h^{-1} and chlorophyll concentration in the euphotic zone reached peaks of 80 µg L^{-1} (Melack, 1982; Melack et al., 1982).

Pelagic biomass (wet weight) reached up to 3 g L^{-1} during a bloom of *Arthrospira fusiformis* (Ballot et al., 2005). Nutrient concentrations (SRP, NH_4^++NH_3, NO_2^- and NO_3^-) are typically lower than 0.4 µM in the mixolimnion, but can rise up at the sediment surface (up to 130 µM and 4000 µM for SRP and NH_4^++NH_3 respectively) (Melack et al., 1982). Chemocline and monimolimnion are anoxic and euxinic, with concentrations of hydrogen sulfide (H_2S) up to 1.2 mM (McIntyre and Melack, 1982).

Verschuren (1999) reported that the uppermost sediment layer, in the 30-50%, consists of highly porous gelatinous organic aggregates of settled decomposing algae and cyanobacteria and that organic carbon represents the 10% of total sediment dry weight (unpublished data from authors).

Sampling was performed on June 18, 2017, in the middle of the lake, at the deepest site. One litre of water was sampled at midday from seven depths: 0, -0.5, -1, -2, -3, -4 and -4.5 m with a Rilsan® tube connected to a syringe with a three-way Teflon valve (Tassi et al., 2004). Sample at 4.5 m depth was collected at the bottom lake at the interface between sediments and water.

2.2. Lake characterization and underwater light attenuation

Water temperature, electrical conductivity, oxidation/reduction potential (ORP), pH and dissolved oxygen profiles were recorded between 3 and 4 p.m. at every 0.5 m, using a YSI Multiparameter probe. ORP was converted into redox potential at 25°C ($E_{0(25^{o}C)}$) according to Wolkersdorfe (2008).

Adsorption spectra between 280 and 1000 nm of unfiltered samples were used to estimate underwater light attenuation spectra at different depths. Underwater light spectra were obtained according to the Beer-Lambert law:

$$I_{\lambda} = I_{0(\lambda)} e^{-z\,\tau_{\lambda}} \qquad (1)$$

Where $I_{0(\lambda)}$ is the input solar intensity at ground level at wavelength λ. τ_{λ} is optical depth at wavelength λ (τ_{λ} =ln(10) Abs_{λ}). Abs_{λ} is the absorbance values at wavelength λ. Spectra were performed with a UV1700 Pharma Spec (Shimadzu) spectrophotometer using a 1-cm quartz cell varying λ between 280 and 1000 nm. The ASTM G173-03 Reference was used as input solar spectrum (http://rredc.nrel.gov/solar/spectra).

2.3. Nutrients, bulk DOM and chromophoric DOM

Water samples (100 mL) were filtered (0.45-µm pore-size nylon filters) and acidified with ultrapure HCl for dissolved inorganic nitrogen (DIN=NH_4^++NH_3+NO_2^-+NO_3^-). NO_2^- and NO_3^- were analyzed with colorimetric method with an autoanalyzer Bran+Luebbe after nitrate reduction with a copper-cadmium column. NH_4^++NH_3 concentrations were estimated with the salicylate method of Reardon (1969). To remove silicate interference, the pH of solution was set to 1. To reduce the interference of salts and sulfite, all samples were previously diluted to 1/10 -1/30.

Dissolved organic carbon (DOC) and total dissolved nitrogen (TDN) were measured by oxidative combustion and infrared analysis using a Shimadzu 5000 A total organic carbon

analyzer coupled to a Total Nitrogen unit. Dissolved organic nitrogen (DON) was calculated as the difference between TDN and DIN.

For DOM quality analysis, water samples (200 mL) were filtered (combusted GFF Whatman filters), acidified with ultrapure HCl (pH =2), and stored in pre-combusted glass bottles.

Samples for spectroscopy were filtered just before their analysis with 0.22-µm-pore nylon membranes to remove particle interferences and, were analyzed at room temperature. Prior any analysis, samples were diluted to 1/25-1/60 (to get a final DOC concentration of 2-4 mg L^{-1}) to attenuate the interference of salinity. Two spectroscopic descriptors were assessed to provide qualitative information about the chromophoric DOM (CDOM), according adsorption spectra of filtered and diluted samples from 200 nm to 800 nm with a UV1700 Pharma Spec (Shimadzu) spectrophotometer using a 1-cm quartz cell. The ultraviolet absorbance $SUVA_{254}$, related to the DOM aromaticity level, was calculated as the absorbance at 254 nm (a_{254}) divided by the DOC concentration and by the cuvette path length (Weishaar et al., 2003). Absorbance spectral slope between 275 and 295 nm was estimated as an indicator of CDOM molecular size, with high values indicating low molecular size and vice versa (Helms et al., 2008). Data were collected in double beam mode using deionized water as the blank.

2.5. Fourier Transform Ion Cyclotron Resonance Mass Spectrometry (FT-ICR-MS).

Filtered acidified water samples (20 mL) were processed through 100 mg styrene-divinyl-polymere type (PPL) solid-phase cartridges (Agilent, Waldbronn, Germany) to desalt the extract (Dittmar et al., 2008) for subsequent electrospray ionization (ESI) mass spectrometry. The solid-phase extracted DOM (SPE-DOM) was eluted twice with 2 mL of methanol. The extracts were diluted with methanol to 5 mL and were kept frozen until analysis (for further details see Raeke et al., 2016). Recovery rates ranged from 30 to 85% being the lowest efficiencies correspond to samples at deepest layers (4 and 4.6 m depth, SI2).

SPE extracts were diluted 1:1 (v/v) with ultrapure water and analyzed with an FT-ICR-MS equipped with a dynamically harmonized analyzer cell (Solari XR, Bruker Daltonics Inc., Billerica, MA) and a 12 T refrigerated actively shielded superconducting magnet (Bruker Biospin, Wissembourg, France). The instrument is located at the ProVIS Centre for Chemical Microscopy within the Helmholtz Centre for Environmental Research. Samples were infused by an autosampler at a flow rate of 10 µL min^{-1}. For each spectrum, 256 scans (ion accumulation time=15 ms) were co-added in the mass range 150-3000 m/z with a 4 MWord time domain. Mass spectra were internally calibrated with a list of peaks (m/z 250-550, n > 110) commonly present in natural organic matter, the mass accuracy after internal linear calibration was better than 0.1 ppm. Peaks were considered if the signal/noise (S/N) ratio was greater than four.

Formulae were assigned to peaks in the mass range 150-700 m/z allowing for elemental compositions $C_{1-60}H_{1-120}O_{1-40}N_{0-2}S_{0-1}$ with an error range of ±0.5 ppm according to Lechtenfeld et al. (2014). Relative peak intensities were calculated based on the summed intensities of all assigned peaks in each sample. As data set detection limit a relative signal intensity of 0.01% was chosen to compensate for variability in sensitivity between different measurements. A molecular formula of a mass peak is referred to as “molecule” in this article although one molecular formula can represent several different structural isomers.

Only formulas with $-10 \leq DBE - O \leq +10$ (DBE: double bound equivalents) were considered for further data evaluation (Herzsprung et al. 2014).

The following descriptors were estimated after molecular formula identification: number of detected molecules (richness) and, molecular mass, H/C, O/C, N/C, S/C, DBE, modified aromaticity index (AImod, Koch and Dittmar, 2016) and nominal oxidation state of carbon (NOSC, LaRowe and Van Cappellen, 2011) weighted averages. C, H, O, N and S refer to the number of atoms of carbon, hydrogen, oxygen, nitrogen and sulfur in each assigned molecule.

The ratio H/C, DBE and AI_{mod} provide information about the degree of saturation of a molecule (i.e. number of C-C double bounds) whereas O/C ratio and NOSC are descriptors of the (average) carbon oxidation state. According to the values of the different DOM indicators, the DOM molecular classes were split into, Carboxyl-rich alicyclic like molecules (CRAM), Aliphatics, Aromatics and Condensed&Aromatic (CA; molecular categories constrains are detailed at Table SI 1). Be aware that each formula can describe numerous isomers this classification suggests the most likely structure (Rossel et al., 2017). CRAM, aliphatic and aromatic molecule are subdivided into O-poor or O-rich molecules if O/C is <0.5 or ≥0.5 respectively.

2.6. Statistics and data analysis

Hierarchical cluster analysis (HCA) of FT-ICR-MS elemental formula data was performed to test differences among samples. HCA included the 2338 components that were common in all samples after ranking the SPE-DOM mass peak intensities for each of the seven samples separately. Squared Euclidean distance with Ward linkage method was applied (Murtagh and Legendre, 2014) by assigning first rank to the variable with the highest intensity.

Inter Sample Rankings Analysis (ISRA) allowed the visualization of DOM quality differences in van Krevelen diagrammes (Herzsprung et al. 2017).

For each SPE-DOM molecular class and descriptor, the weighted average was estimated from relative intensity of the peak of each assigned molecule.

At Sonachi, the water column showed a meromictic stratification with a chemocline that separate two main water masses: mixolimnion and monimolimnion (details in the results section).

A simple end-member mixing model was used to quantify the magnitude of mixing at chemocline, according to the following mass balance:

$$y = \frac{C_{ch} - C_{mix}}{C_{mon} - C_{mix}} \quad (2)$$

$$y + x = 1$$

x and y are the relative contributions of mixolimnion and monimolimnion. C_{ch}, C_{mix} and C_{mon} are the measured tracer concentrations (conservative solute) at chemocline, mixolimnion and monimolimnion respectively. C_{mix} represented the average value of the tracer concentrations between surface (0 m) and 3 m depth (n=5). Specific electrical conductivity at 20°C was adopted as conservative tracer (Leibundgut et al., 2011).

Calculation of the magnitude of mixing (i.e. x and y in eq. 2) allowed the estimation of the expected concentration of a reactive solute at the chemocline ($RS_{(exp;ch)}$):

$$RS_{(exp;ch)} = x\, RS_{(mix)} + y\, RS_{(mon)} \quad (3)$$

where $RS_{(mix)}$ and $RS_{(mon)}$ are the measured concentrations of a reactive solute at mixolimnion and monimolimnion respectively.

Differences between expected and observed values provided a quantitative information (η) about net retention or release of a reactive solute at the chemocline:

$$\eta = \frac{(RS_{(obs;ch)} - RS_{(exp;ch)})}{RS_{(exp;ch)}} * 100 \quad (4)$$

If η>0 (or η<0) the reactive solute was released (or retained) at chemocline (Butturini et al., 2016). Mass balance was performed for DOC and DON.

3. Results

3.1. Limnologic characterization

Temperature and oxygen in the water column ranged between 20.5 and 22.4^{o}C, and <10^{-3} and 0.1 mM (0-43% of saturation), respectively. A sharp change denoted the presence of a thermocline and an oxycline at 1.5 m depth. pH was almost steady at 9.6 from surface down to 3 m depth, but decreased slightly to 9.5 below 4 m. Specific electrical conductivity was homogeneous (*ca.* 9.8 mS cm^{-1}) from the surface to 3 m depth and increased rapidly to 11.5 and 16.2 mS cm^{-1} at 4 m and at the bottom (i.e. sediment-water interface). The vertical profile of redox potential ($E_{0(25^{o}C)}$) showed a complex pattern: its value was steady at 298 mV in the first 1.5 m, then it gradually decreased to 140 mV at 3 m depth, and finally decreased abruptly to less than -64 mV below 4 m. Overall, vertical profiles of pH, specific electrical conductivity and $E_{0(25^{o}C)}$, revealed the presence of a chemocline at about 3.5-4 m depth that separated a mixolimnion from a monimolimnion (Figures 1a-e). According to the mixing model, 74.2% of the water at chemocline came from mixolimnion and the rest from the monimolimnion. DIN concentration averaged 1.8±1.2 μM N and did not show any clear vertical trend (Table SI3).

3.2. Light regime in water column.

According to the adsorption spectra measured in unfiltered samples, 99% of the total radiation was absorbed within the oxycline; at chemocline darkness was total (**Figure SI2**). UVA and UVB radiation disappeared within the first 25 cm (Figure 1f).

3.3. DOC, DON and CDOM

Dissolved organic carbon (DOC) averaged 8.1±0.8 mM in the mixolimnion and increased to 48.8 mM in the monimolimnion (Figure 1g). Total dissolved organic nitrogen (DON) averaged 800±90 μM in the mixolimnion and increased in the monimolimnion (Figure 1h). DOC and DOM showed similar vertical profiles. However DOC/DON ratio was not steady and showed an abrupt decline from 8.8 at mixolimnion, to 1.8 at the chemocline. The mass balance revealed

that the chemocline was a highly reactive site for DOM; while DOC was retained (η=-47%), DON was released (η=105%; Figures 1g-h). $SUVA_{254}$ was almost constant in mixolimnion (4.5±0.3 mgC L/m) but it dropped to <1 mgC L m^{-1} at monimolimnion (Figure 1i). On the other hand, spectral Slope $S_{275-295}$, oscillated widely, without a clear vertical gradient with a subtle accumulation of relatively larger molecules at chemocline and smaller ones at 0,5 m depth respectively.

3.4. SPE-DOM

FT-ICR-MS detected 6221 elemental formulae. A subtotal of 2338 formulae were shared between all seven samples. Number of identified formulae in each sample oscillated between 3449 and 4344 (Table SI1).

The most abundant compositional group (39-49% of relative peak intensity) was represented by O-poor CRAM-like molecules, structurally similar to sterols and hopanoids (Hertkorn et al., 2006). Aromatics and Condensed&Aromatics (CA, resulting from vascular plant leaching/degradation, Kellerman et al., 2015) were much lower and comprised between 1.5 to 4.2% of the total signal. Aromatic O-poor molecules were slightly more abundant than the O-rich fraction. Aliphatic molecules were also relevant, contributing 12.3-19.6% of the total peak intensity with the O-poor fraction being four times more intense (Table 2).

HCA of SPE-DOM data highlighted the impact of water stratification on DOM; the sample at chemocline resulted the most dissimilar one (Figure 2).

Van Krevelen space visually illustrated how SPE-DOM differed across samples (Figure 2). The chemocline sample showed relatively high peak intensities (ranks 1 and 2) in the region H/C>1 and O/C<0.6. In contrast, the weakest peaks (ranks 6 and 7) were preferentially located at O/C>0.5.

In the monimolimnion, the most intense peaks were mainly located at H/C>1.2 and 0.2<O/C<0.8. Meanwhile the weakest ones were for molecules with 1< H/C < 1.5 and 0.2 < O/C < 0.6.

In the mixolimnion, at depths 0.5, 1, 2 and 3 m, the most intense signal was related to molecules with H/C<1.4 and O/C>0.4. In surface water, the distribution of ranks in the van Krevelen diagram differed a little from that at the mixolimnion and the most intense peaks shift slightly to the region H/C<1.5 and 0.2<O/C<0.5.

At the chemocline and the bottom, the 30 and 38.7% of cases with rank 1 and 2 (i.e. the relatively high peak intensities) were located in the region H/C>1.5 and 0.2<O/C<0.53 of the van Krevelen diagram. This percentage dropped to less than 3.8% in the mixolimnion samples. Within the mixolimnion, the 80-86% of cases with rank 1 and 2 were located in the region 0.65<H/C<1.5 and 0.25<O/C<0.67. This percentage decreased to less than 63% at the chemocline and within the monimolimnion.

At the lake bottom, under permanent darkness, anoxic and reduced conditions, organic rich sediments released a large amount (DOC~50 mM) of DOM enriched in highly reduced (NOSC<-0.38, Figure 3a) and saturated (DBE<6.8; Figure 3b), O-poor aliphatic and CRAM molecules (Figure 3c-d), and strongly depleted in aromatic ones (Figure 3e).

HCA (Figure 2) also suggested that SPE-DOM at the surface (0 m) differed slightly from the rest of samples of the mixolimniom. More specifically, at surface, the relative intensity of SPE-DOM molecules that were slightly more aliphatic (higher H/C, Mann Whitney U test, p<0.0001) and more reduced (lower O/C and lower NOSC, Mann Whitney test, p<0.0001; Figure SI7**)** increased**.**

Non-oxygen heteroatom molecules (CHN_1O, CHN_2O, CHOS, and CHNOS) represented 51.3 - 53.4% of the total of the molecules identified (Table SI2 and Figure SI 3-6). N-bearing molecules were especially relevant representing 40±0.9% of SPE-DOM molecules with a

relative signal intensity averaging 18.5±1.2%. On the other hand, S-bearing molecules were less relevant (7.8±3.6% of SPE-DOM molecules and 3.5±0.7% of relative intensity). CHNO and CHOS were smaller (lower molecular mass), more oxidized (higher NOSC) and less aromatic (lower AImod) than CHO molecules (Figure SI8).

4. Discussion

Vertical profiles of chemical and physical properties of lake water (Electrical conductivity, Oxygen, pH and light extinction rate) reported in the present study were similar to those reported in previous studies (Melack et al., 1982; Melack and MacIntyre, 2016) evidencing that meromixis is common at Sonachi. The high radiation extinction rate could reflect the abundance of pelagic algal biomass (e.g. cyanobacteria; Ballot et al., 2005) and the large amount of DOM suggesting that its photo-degradation is effective only within the first few centimeters of the water column.

DOC concentrations within the water column were 1-2 orders of magnitude higher than those typically reported for freshwaters (Sobek et al., 2007; Chen et al., 2015) and even slight higher than those reported for endorheic saline waters around the world (Song et al., 2019; Osburn et al., 2011; Mariot et al, 2007).

SPE-DOM showed marked differences with in respect to what is usually reported in inland waters. Contributions of CRAM and aromatics were remarkably lower respect to (Riedel et al., 2016; Stubbins et al., 2006), while aliphatics were significantly higher (Figure 4). Higher and comparable aliphatic relative contributions were reported only in a coastal Antarctic pond (i.e. Pony lake, Kellerman et al., 2018) and in a tropical reservoir during a cyanobacterial bloom (Bittar et al., 2015), respectively. Overall, SPE-DOM at Sonachi was more reduced, less aromatic and more saturated than typical SPE-DOM from inland waters (Raeke et al., 2017; Dadi et al., 2017; Kellerman et al., 2018).

The relative low contribution of aromatics and CA pointed to the presence of highly degraded and processed DOM, altered by intense photodegradation (Stubbins et al., 2006; Bittar et al., 2015). The relatively high abundance of aliphatics might reflect DOM release from pelagic cyanobacteria (Welker and Von Dohren, 2006; Biller et al., 2015). Aliphatics are considered to be unaffected by photodegradation (Stubbins et al., 2006; Timko et al., 2015) and their relative relevance might have been additionally amplified by the photodegradation of aromatics.

At mixolimniom, SPE-DOM properties were homogeneous thus evidencing a rapid mixing between the most superficial and oxic layer and the underneath anoxic mixolimnion. A subtle change was detected at surface with a slight relative accumulation of O-poor CRAM and O-poor aliphatic compounds together to a relative decrease of O-rich aromatics (Figure 3). These small molecular shifts, in comparison to the rest of the mixolimnion, might be attributable to photo decarboxylation of O-rich aromatic molecules (Lv et al., 2017), suggesting that photodegradation might be limited to thet first few centimeters of the water column as suggested by underwater UVA and UVB vertical profiles (Figure 1e).

Interestingly, most SPE-DOM descriptors (i.e. $NOSC_w$, $Mass_w$, $Aliphatic_w$, $Aromatic_w$, O/C_w, H/C_w; Table 1 and Figures 3) showed abrupt changes at chemocline. This finding, together with DOM mass balance estimates, evidenced that the chemocline was a site of remarkable readjustment of DOM concentration and of the SPE-DOM molecular signature.

At the bottom and at the chemocline, the additional increase in the relative contribution of saturated O-poor aliphatics was interpreted to reflect the release of microbially derived DOM (Lechtenfeld et al., 2015) and the degradation of cyanobacteria/algae detritus accumulated at the sediments-water interface (Verschuren, 1999). The abundance of aliphatic substances at the lake bottom might be even larger than that detected by FT-ICR-MS analyses. Raeke et al. (2016) reported that PPL sorbents are less efficient in retaining O-poor (O/C<0.4) and saturated (i.e. H/C>1.5) molecules. DOM recovery rates of SPE extractions in samples collected at the

bottom and at the chemocline (appendix Table SI1) were lower compared to the samples from the mixolimnion. Consequently, a large fraction of aliphatic compounds might be missing in the MS analysis of bottom waters. Additionally, highly reduced conditions at the bottom together with high pH probably boosted DOM release because of the deprotonation of mineral sediments with subsequent reduction of their DOM adsorption potential (Grybos et al., 2009).

Organic rich sediment of SLAR host a highly complex and unique consortium of alkaliphilic prokaryotes (Grant and Jones, 2016). Almost nothing is known about the magnitude of their in-situ activities but a rough idea can be deduced from Ceiling (1996) who reported values of δ^{13}CDIC signatures higher than +10‰ in interstitial water pointing to the occurrence of high microbial activities. Therefore, the high contribution of O-poor saturated aliphatic substances in out the bottom samples is likely a signature of high microbial activity at the sediment-water interface.

FT-ICR-MS has been extensively used to explore SPE-DOM chemodiversity across lakes at regional scale (Kellerman et al., 2015), but the impact of lake stratification on DOM molecular signatures is almost overlooked . Dadi et al. (2017) reported that in a reservoir, with a DOC/Fe molar ratio of around 40, the unsaturated and O-rich SPE-DOM components were adsorbed onto ferric iron minerals under epilimnetic oxic conditions and were released under anoxic and reduced conditions at the sediments following reduction of solid ferric iron to soluble ferrous iron. At Lake Sonachi the DOM absorption/desorption processes related to iron redox cycling appeared to be less relevant because the oxic conditions persisted only in the first meter of the water column. Further, total dissolved iron concentration in water was below 0.7 µM (unpublished data from authors) and the DOC/Fe molar ratio was higher than 10000. In consequence the influence of adsorption/desorption processes of unsaturated and O-rich DOM bound to ferric iron minerals can be considered negligible.

Regarding to non-oxygen heteroatomic molecules, the relative intensity of N-bearing molecules was about 3-4 times higher than that reported in large rivers and it was in the same range of that measured in ancient ocean waters (Riedel et al., 2016) and in submarine hydrothermal fluids (Gomez-Saez et al., 2016). On the other side, the percentage of CHOS molecules was similar to that reported in freshwaters (Riedel et al., 2016, Kellermann et al., 2018) but much lower than in hydrothermal fluids with evidence of abiotic sulfurization by H_2S (Gomez-Saez et al., 2016) or in sewage sludge waters (Lv et al., 2017). Further, CHOS molecules tend to be slightly smaller and more oxidized that CHO molecules suggesting that abiotic sulfurisation of CHO molecules seemed to be unimportant (Melendez-Perez et al., 2018).

5. Conclusions and implications

DOM is a fundamental component of the study of the carbon cycle in the hydrosphere (Dittmar and Stubbins, 2014; McCallister et al., 2018). Apart from few remarkable exceptions (Waiser and Robarts, 2000; Mariot et al, 2007, Osburn et al., 2011, Song et al., 2019), DOM in saline-alkaline endorheic systems has attracted little attention and these ecosystems are missing in reviews focused on DOM quantity and quality in inland waters worldwide (Sobek et al., 2007; Alvarez-Cobelas et al., 2012; Chen et al., 2015; Kellerman et al., 2018). Thus, the SLARs, the most productive waterbodies worldwide (Lewis, 2011), are not taken into account in these global assessments.

In conclusion our study reveals that:

- SLARs provide unique reservoirs of microbially derived, photodegraded, little aromatic and saturated O-poor DOM suggesting that a full understanding of the processes governing DOM availability and properties in inland waters (Sobek et al., 2007; Chen et al., 2015; Kellermann et al., 2015) needs to include a recognition of the processes taking place in endorheic saline-alkaline lakes characterized by a high productivity.

- The DOM molecular signature in endorheic saline-alkaline Lake Sonachi reflected the pressure exerted by photodegradation acting at the same time as microbial production and degradation. Photodegradation might be at work within the first few centimeters of the water surface, while the greatest changes in quantity, reactivity and molecular signature were located at the chemocline under steep geochemical gradients.

- These findings emphasize that, next to regional-scale climatic and hydrological drivers, small-scale internal discontinuities create striking changes in the DOM molecular signatures of lentic waters.

Acknowledgements

Authors thank Tina Kuhar for DOM analysis. We gratefully acknowledge Jan Kaesler for his help with the FT-ICR-MS and the Centre for Chemical Microscopy (ProVIS) at the Helmholtz Centre for Environmental Research, Leipzig (Germany), supported by European Regional Development Funds (EFRE - Europe funds Saxony) and the Helmholtz Association. We thank the Spanish Ministry of Ministerio de Ciencia, Innovación y Universidades (Project DRYHARHSAL, RTI2018-097950-B-C21) and the European Union 7th Framework Programme (Project No. 603629-ENV-2013-6.2.1-Globaqua) projects for funding FT-ICR-MS analysis. Authors are grateful to the Sonachi Lodge Manager, Lawi Kiplimo for facilitating access to the site and to Michael Schägerl for suggestions in an early draft of the manuscript. This study has been performed under research clearance permit NACOSTI/P/16/23342/10489 *Biodiversity studies in Kenya's Rift Valley*, granted by the Government of Kenya.

References

Alvarez-Cobelas, M., Angeler, D. G., Sánchez-Carrillo, S., & Almendros, G., 2012. A worldwide view of organic carbon export from catchments. Biogeochemistry, 107, 275-293.

Ballot, A., Krienitz, L., Kotut, K., Wiegand, C., & P flugmacher, S., 2005. Cyanobacteria and cyanobacterial toxins in the alkaline crater lakes Sonachi and Simbi, Kenya. Harmful algae, 4, 139-150.

Biller, P., Ross, A. B., & Skill, S. C., 2015. Investigation of the presence of an aliphatic biopolymer in cyanobacteria: Implications for kerogen formation. Organic Geochemistry, 81, 64-69.

Bittar, T. B., Stubbins, A., Vieira, A. A., & Mopper, K., 2015. Characterization and photodegradation of dissolved organic matter (DOM) from a tropical lake and its dominant primary producer, the cyanobacteria Microcystis aeruginosa. Marine Chemistry, 177, 205-217.

Butturini, A., Guarch, A., Romaní, A. M., Freixa, A., Amalfitano, S., Fazi, S., & Ejarque, E., 2016. Hydrological conditions control in situ DOM retention and release along a Mediterranean river. Water Research, 99, 33-45.

Cerling, T. E., 1996. Pore water chemistry of an alkaline lake: Lake Turkana, Kenya. Limnology, Climatology and Paleoclimatology of the East African Lakes, 225, 240.

Chen, M., Zeng, G., Zhang, J., Xu, P., Chen, A., & Lu, L., 2015. Global landscape of total organic carbon, nitrogen and phosphorus in lake water. Scientific Reports, 5, 15043.

Dadi, T.; Harir, M.; Hertkorn, N.; Koschorreck, M.; Schmitt-Kopplin, P.; Herzsprung, P., 2017. Redox conditions affect DOC quality in stratified freshwaters. Environ. Sci. Technol., 51, 13705-13713.

Dittmar, T., & Stubbins, A., 2014. 12.6—Dissolved organic matter in aquatic systems. Treatise on Geochemistry, 2nd edn. Elsevier: Oxford, p. 125-156.

Dittmar, T., Koch, B., Hertkorn, N., & Kattner, G., 2008. A simple and efficient method for the solid-phase extraction of dissolved organic matter (SPE-DOM) from seawater. Limnol. Ocean. Methods, 6(6), 230-235.

Dodds, W. K. and Whiles, M.R., 2002. Freshwater ecology: concepts and environmental applications of limnology. 2nd edn. Academic press. p. 829

Elkins, K. M., & Nelson, D. J., 2002. Spectroscopic approaches to the study of the interaction of aluminum with humic substances. Coord. Chem. Rev., 228, 205-225.

Gaudet, J. J., & Melack, J. M., 1981. Major ion chemistry in a tropical African lake basin. Freshwater Biology, 11, 309-333.

Gomez-Saez, G. V., Niggemann, J., Dittmar, T., Pohlabeln, A. M., Lang, S. Q., Noowong, A., ... & Bühring, S. I., 2016. Molecular evidence for abiotic sulfurization of dissolved organic matter in marine shallow hydrothermal systems. Geochim. Cosmochim, Acta, 190, 35-52.

Gonsior, M., Peake, B. M., Cooper, W. T., Podgorski, D., D'Andrilli, J., & Cooper, W. J., 2009. Photochemically induced changes in dissolved organic matter identified by ultrahigh resolution Fourier transform ion cyclotron resonance mass spectrometry. Environ. Sci. Technol., 43, 698-703.;

Grant, W. D., & Jones, B. E., 2016. Bacteria, archaea and viruses of soda lakes. In *Soda Lakes of East Africa*. Springer, Cham. pp. 97-147

Grybos, M., Davranche, M., Gruau, G., Petitjean, P., & Pédrot, M., 2009. Increasing pH drives organic matter solubilization from wetland soils under reducing conditions. Geoderma, 154, 13-19.

Hecky, R. E., & Kilham, P., 1973. Diatoms in alkaline, saline lakes: ecology and geochemical implications 1. Limnol. Oceanogr., 18, 53-71.

Helms, J. R., Stubbins, A., Ritchie, J. D., Minor, E. C., Kieber, D. J., & Mopper, K., 2008. Absorption spectral slopes and slope ratios as indicators of molecular weight, source, and photobleaching of chromophoric dissolved organic matter. *Limnology and Oceanography*, *53*(3), 955-969.

Hertkorn, N., Benner, R., Frommberger, M., Schmitt-Kopplin, P., Witt, M., Kaiser, K., ... & Hedges, J. I., 2006. Characterization of a major refractory component of marine dissolved organic matter. Geochim. Cosmochim, Acta, 70, 2990-3010.

Herzsprung, P., Hertkorn, N., von Tümpling, W., Harir, M., Friese, K., & Schmitt-Kopplin, P. (2014). Understanding molecular formula assignment of Fourier transform ion cyclotron resonance mass spectrometry data of natural organic matter from a chemical point of view. Anal. Bioanal. Chem., 406(30), 7977-7987.

Herzsprung, P., Osterloh, K., von Tümpling, W., Harir, M., Hertkorn, N., Schmitt-Kopplin, P.,Meissner, R., Bernsdorf, S., Friese,K. (2017). Differences in DOM rewetted and natural peatlends- results from FT-ICR-MS and bulk optical parameters. STOTEN, 586, 770-781.

Jirsa, F., Gruber, M., Stojanovic, A., Omondi, S. O., Mader, D., Körner, W., & Schagerl, M. (2013). Major and trace element geochemistry of Lake Bogoria and Lake Nakuru, Kenya, during extreme drought. Chem. Erde-Geochem., 73, 275-282.

Kilham P, Kilham SS., 1989. Endless summer: internal loading processes dominate nutrient cycling in tropical lakes. Freshwater Biol. 23:379-389.

Kellerman, A. M., Guillemette, F., Podgorski, D. C., Aiken, G. R., Butler, K. D., & Spencer, R. G., 2018. Unifying concepts linking dissolved organic matter composition to persistence in aquatic ecosystems. Environ. Sci. Technol., *52*, 2538-2548.

Kellerman, A. M., Kothawala, D. N., Dittmar, T., & Tranvik, L. J., 2015. Persistence of dissolved organic matter in lakes related to its molecular characteristics. Nat. Geo., 8, 454.

Koch, B. P., and Dittmar, T., 2016. Erratum: From mass to structure: an aromaticity index for high-resolution mass data of natural organic matter. Rapid Comm. Mass Spectrom., 30, 250. doi: 10.1002/rcm.7433

LaRowe, D. E., & Van Cappellen, P., 2011. Degradation of natural organic matter: a thermodynamic analysis. Geochim. Cosmochim, Acta, 75, 2030-2042.

Lechtenfeld, O. J., Kattner, G., Flerus, R., McCallister, S. L., Schmitt-Kopplin, P., & Koch, B. P., 2014. Molecular transformation and degradation of refractory dissolved organic matter in the Atlantic and Southern Ocean. Geochim. Cosmochim, Acta, 126: 321-337.

Lechtenfeld, O.J.; Hertkorn, N.; Shen, Y.; Witt, M.; Benner, R., 2015. Marine sequestration of carbon in bacterial metabolites. Nat. Commun. 6:6711.

Leibundgut, C., Maloszewski, P., & Külls, C., 2011. Tracers in hydrology. John Wiley & Sons. P. 415.

Leinemann, T., Preusser, S., Mikutta, R., Kalbitz, K., Cerli, C., Höschen, C., ... & Guggenberger, G., 2018. Multiple exchange processes on mineral surfaces control the transport of dissolved organic matter through soil profiles. Soil Biol. Biochem., 118, 79-90.

Lewis Jr, W. M., 2011. Global primary production of lakes: 19th Baldi Memorial Lecture. Inland Waters, 1, 1-28.

Lv, J., Li, D., Lou, L., wu, T. & Zhang, S., 2017. Molecular transformation of natural and anthropogenic dissolved organic matter under photo-irradiation in the presence of nano TiO_2. Wat. Res., 125: 201-208.

MacIntyre, S., & Melack, J. M., 1982. Meromixis in an equatorial African soda lake 1. Limnol. Oceanogr., 27, 595-609.

Massicotte, P., Asmala, E., Stedmon, C., & Markager, S., 2017. Global distribution of dissolved organic matter along the aquatic continuum: Across rivers, lakes and oceans. STOTEN, 609, 180-191.

McCallister, S. L., Ishikawa, N. F., & Kothawala, D. N., 2018. Biogeochemical tools for characterizing organic carbon in inland aquatic ecosystems. Limnol. Oceanogr. Letters, 3, 444-457.

Mariot, M., Dudal, Y., Furian, S., Sakamoto, A., Vallès, V., Fort, M., & Barbiero, L., 2007. Dissolved organic matter fluorescence as a water-flow tracer in the tropical wetland of Pantanal of Nhecolândia, Brazil. STOTEN, 388, 184-193.

Melack, J. M., & MacIntyre, S., 2016. Morphometry and Physical Processes of East African Soda Lakes. In *Soda Lakes of East Africa* (pp. 61-76). Springer, Cham.

Melack, J. M., 1982. Photosynthetic activity and respiration in an equatorial African soda lake. Freshwat. Biol., 12, 381-400.

Melack, J. M., Kilham, P., & Fisher, T. R., 1982. Responses of phytoplankton to experimental fertilization with ammonium and phosphate in an African soda lake. Oecologia, 52, 321-326.

Melendez-Perez, J. J., Martinez-Mejia, M. J., Barcellos, R. L., Fetter-Filho, A. F., & Eberlin, M. N., 2018. A potential formation route for CHOS compounds in dissolved organic matter. Mar. Chem., 202, 67-72.

Meybeck, M., 1995. Global distribution of lakes. In Physics and chemistry of lakes. Springer, Berlin, Heidelberg. p. 1-35

Murtagh, F., & Legendre, P., 2014. Ward's hierarchical agglomerative clustering method: which algorithms implement Ward's criterion?. J. Class., 31(3), 274-295.

Odongo, V. O., van der Tol, C., Becht, R., Hoedjes, J. C., Ghimire, C. P., & Su, Z., 2016. Energy partitioning and its controls over a heterogeneous semi-arid shrubland ecosystem in the Lake Naivasha Basin, Kenya. Ecohydrology, 9, 1358-1375.

Oduor, S. O., & Schagerl, M., 2007. Phytoplankton primary productivity characteristics in response to photosynthetically active radiation in three Kenyan Rift Valley saline–alkaline lakes. J. Plankton Res., 29, 1041-1050.

Olaka, L. A. (2011). Hydrology across scales: sensitivity of East African lakes to climate changes. PhD thesis.

Osburn, C. L., Wigdahl, C. R., Fritz, S. C., & Saros, J. E., 2011. Dissolved organic matter composition and photoreactivity in prairie lakes of the US Great Plains. Limnol. Oceanogr., 56, 2371-2390.

Riedel, T., Zark, M., Vähätalo, A. V., Niggemann, J., Spencer, R. G., Hernes, P. J., & Dittmar, T., 2016. Molecular signatures of biogeochemical transformations in dissolved organic matter from ten world rivers. Front. Earth Sci., 4, 85.

Raeke, J., Lechtenfeld, O. J., Tittel, J., Oosterwoud, M. R., Bornmann K., and Reemtsma, T., 2017. Linking the mobilization of dissolved organic matter in catchments and its removal in drinking water treatment to its molecular characteristics. Water Research 113: 149-159

Raeke, J., Lechtenfeld, O.J., Wagner, M., Herzsprung, P., Reemtsma, T., 2016. Selectivity of solid phase extraction of freshwater dissolved organic matter and its effect on ultrahigh resolution mass spectra. Environ. Sci. Processes & Impacts, 18, 918 – 927.

Reardon, J., 1969. Salicylate method for the quantitative determination of ammonia nitrogen U.S. Patent No. 3,432,395. Washington, DC: U.S. Patent and Trademark Office.

Rossel, P. E., Stubbins, A., Rebling, T., Koschinsky, A., Hawkes, J. A., & Dittmar, T., 2017. Thermally altered marine dissolved organic matter in hydrothermal fluids. Organic geochemistry, 110: 73-86.

Salm, C. R., Saros, J. E., Fritz, S. C., Osburn, C. L., & Reineke, D. M., 2009. Phytoplankton productivity across prairie saline lakes of the Great Plains (USA): a step toward deciphering patterns through lake classification models. Can. J. Fish. Aquat. Sci., *66*(9), 1435-1448.

Schagerl, M. (Ed.)., 2016. Soda Lakes of East Africa. Berlin: Springer.p. 408

Sobek, S., Tranvik, L. J., Prairie, Y. T., Kortelainen, P., & Cole, J. J., 2007. Patterns and regulation of dissolved organic carbon: An analysis of 7,500 widely distributed lakes. Limnol. Oceanogr., 52, 1208-1219.

Song, K., Shang, Y., Wen, Z., Jacinthe, P. A., Liu, G., Lyu, L., & Fang, C., 2019. Characterization of CDOM in saline and freshwater lakes across China using spectroscopic analysis. *Water research*, *150*, 403-417.

Stubbins, A., Spencer, R. G., Chen, H., Hatcher, P. G., Mopper, K., Hernes, P. J., ... & Six, J., 2010. Illuminated darkness: molecular signatures of Congo River dissolved organic matter and its photochemical alteration as revealed by ultrahigh precision mass spectrometry. Limnol. Oceanogr., 55, 1467-1477.

Stubbins, A., Uher, G., Law, C. S., Mopper, K., Robinson, C., & Upstill-Goddard, R. C., 2006. Open-ocean carbon monoxide photoproduction. Deep Sea Research Part II: Tropical Studies in Oceanography, *53*(14-16), 1695-1705.

Talling, J. F., 2011. Some distinctive subject contributions from tropical Africa to fundamental science of inland waters. Inland Waters, 1, 61-73.

Talling, J. F., Wood, R. B., Prosser, M. V., & Baxter, R. M., 1973. The upper limit of photosynthetic productivity by phytoplankton: evidence from Ethiopian soda lakes. Freshwater Biol., 3, 53-76.

Tassi, F., Fazi, S., Rossetti, S., Pratesi, P., Ceccotti, M., Cabassi, J., ... & Vaselli, O. (2018). The biogeochemical vertical structure renders a meromictic volcanic lake a trap for geogenic CO_2 (Lake Averno, Italy). PloS one, 13, e0193914.

Tassi, F., Vaselli, O., Giannini, L., Tedesco, D., Nencetti, A., Montegrossi, G., & Yalire, M. M. 2004. A low-cost and effective method to collect water and gas samples from stratified crater lakes: the 485 m deep lake Kivu (DRC). Proc. IAVCEI Gen. Ass., Puchon, Chile, p. 14-19.

Thrane, J. E., Hessen, D. O., & Andersen, T. 2014. The adsorption of light in lakes: negative impact of dissolved organic carbon on primary productivity. Ecosystems, 17, 1040-1052.

Timko, S. A., Maydanov, A., Pittelli, S. L., Conte, M. H., Cooper, W. J., Koch, B. P., ... & Gonsior, M., 2015. Depth-dependent photodegradation of marine dissolved organic matter. *Front. Mar. Sci.*, *2*, 66.

Verschuren, D. (1999). Influence of depth and mixing regime on sedimentation in a small, fluctuating tropical soda lake. Limnol. Oceanogr., 44, 1103-1113.

Waiser, M. J., & Robarts, R. D., 2000. Changes in composition and reactivity of allochthonous DOM in a prairie saline lake. Limnol. Oceanogr., 45, 763-774.

Weishaar, J. L., Aiken, G. R., Bergamaschi, B. A., Fram, M. S., Fujii, R., & Mopper, K., 2003. Evaluation of specific ultraviolet absorbance as an indicator of the chemical composition and reactivity of dissolved organic carbon. Environ. Sci. Technol., 37, 4702-4708

Welker, M., & Von Döhren, H., 2006. Cyanobacterial peptides—nature's own combinatorial biosynthesis. FEMS microbiology reviews, 30, 530-563.

Wolkersdorfer, C., 2008. *Water management at abandoned flooded underground mines: fundamentals, tracer tests, modelling, water treatment*. Springer Science & Business Media.

Wurtsbaugh, W. A., Miller, C., Null, S. E., DeRose, R. J., Wilcock, P., Hahnenberger, M., ... & Moore, J., 2017. Decline of the world's saline lakes. Nat. Geo., 10(11), 816.

Zinabu, G. M., & Taylor, W. D. (1997). Bacteria—chlorophyll relationships in Ethiopian lakes of varying salinity: are soda lakes different?. J. Plankton Res., 19, 647-654.

Table 1. SPE-DOM molecular characterization at Sonachi. Molecular class criteria and SPE-DOM descriptors are defined at table SI1. All values are signal intensity weighted. CA: Condensed and aromatic.

Depth (m)	CRAM		Aliphatic		Aromatic		CA
	O poor	O rich	O poor	O rich	O poor	O rich	
0	41.85	18.15	10.05	2.21	2.47	1.52	0.90
0.5	39.54	19.36	9.25	2.11	2.42	1.72	0.85
1	40.40	18.80	9.55	2.18	2.35	1.67	0.88
2	40.02	19.05	9.50	2.19	2.38	1.68	0.87
3	40.02	18.79	9.47	2.38	2.36	1.59	0.87
4	49.13	9.79	16.81	2.82	1.23	0.23	0.16
4.5	39.59	16.15	12.60	2.94	1.59	0.63	0.29

Depth (m)	# of molecules	$Mass_w$ (Da)	$NOSC_w$	$AImod_w$	DBE_w	C_w	N_w	S_w	O/C_w	H/C_w	S/C_w	N/C_w
0	4207	356.6	-0.336	0.227	7.092	17.16	0.24	0.03	0.46	1.31	0.0019	0.0155
0.5	3701	355.6	-0.310	0.225	7.117	16.98	0.26	0.04	0.47	1.30	0.0036	0.0172
1	3809	355.7	-0.318	0.227	7.105	17.03	0.25	0.04	0.46	1.30	0.0032	0.0163
2	4208	357.1	-0.314	0.225	7.122	17.07	0.25	0.04	0.47	1.30	0.0030	0.0165
3	4344	357.4	-0.317	0.225	7.114	17.11	0.25	0.03	0.47	1.30	0.0025	0.0165
4	3948	365.0	-0.499	0.194	6.758	18.02	0.21	0.04	0.42	1.38	0.0034	0.0132
4.5	3449	354.4	-0.379	0.200	6.724	17.03	0.25	0.03	0.46	1.35	0.0023	0.0163

Figures

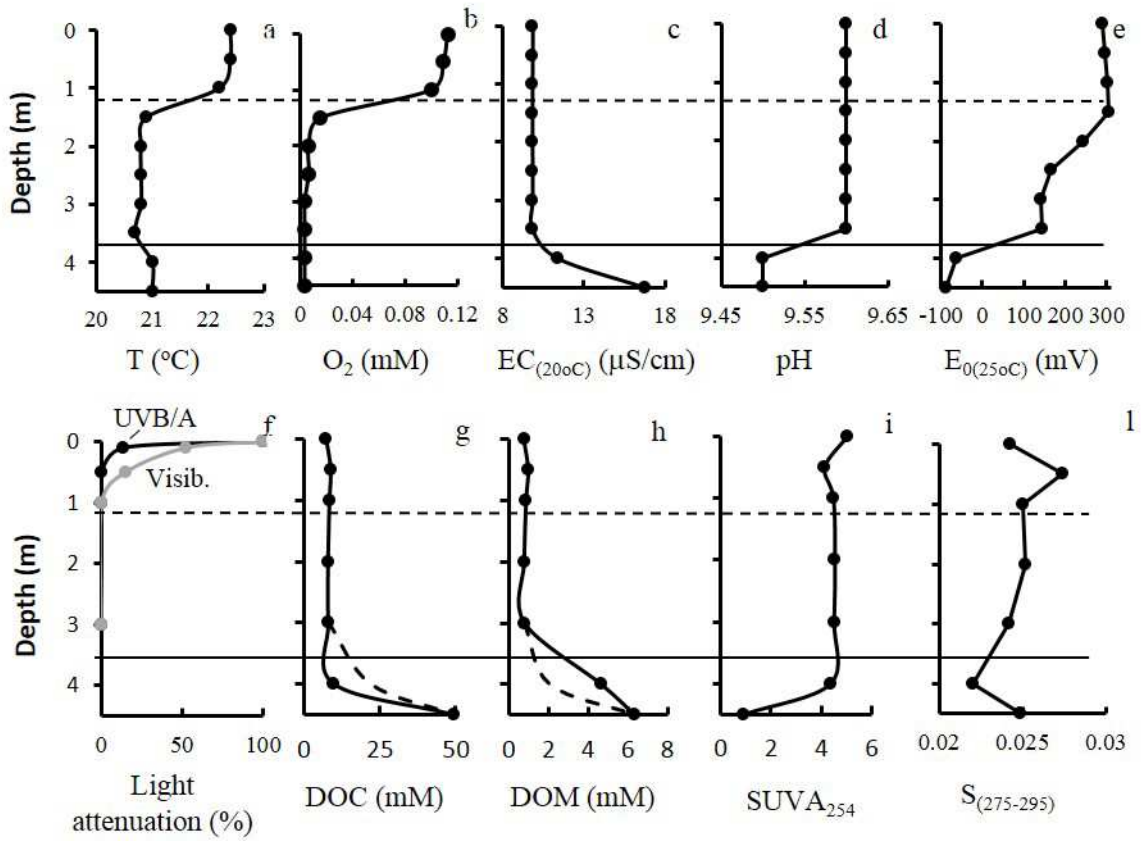

Figure 1. Vertical profiles of water temperature, dissolved oxygen, Electrical conductivity (EC), pH, E_0, underwater light attenuation, DOC, DON, $SUVA_{254}$ and $S_{(275-295)}$. Dashed curves in the lower portion of panels *g* and *h* show expected trends assuming conservative solute mixing between mixolimnion and monimolimnion. Horizontal lines indicate depths of thermocline/oxycline (dashed) and chemocline (solid).

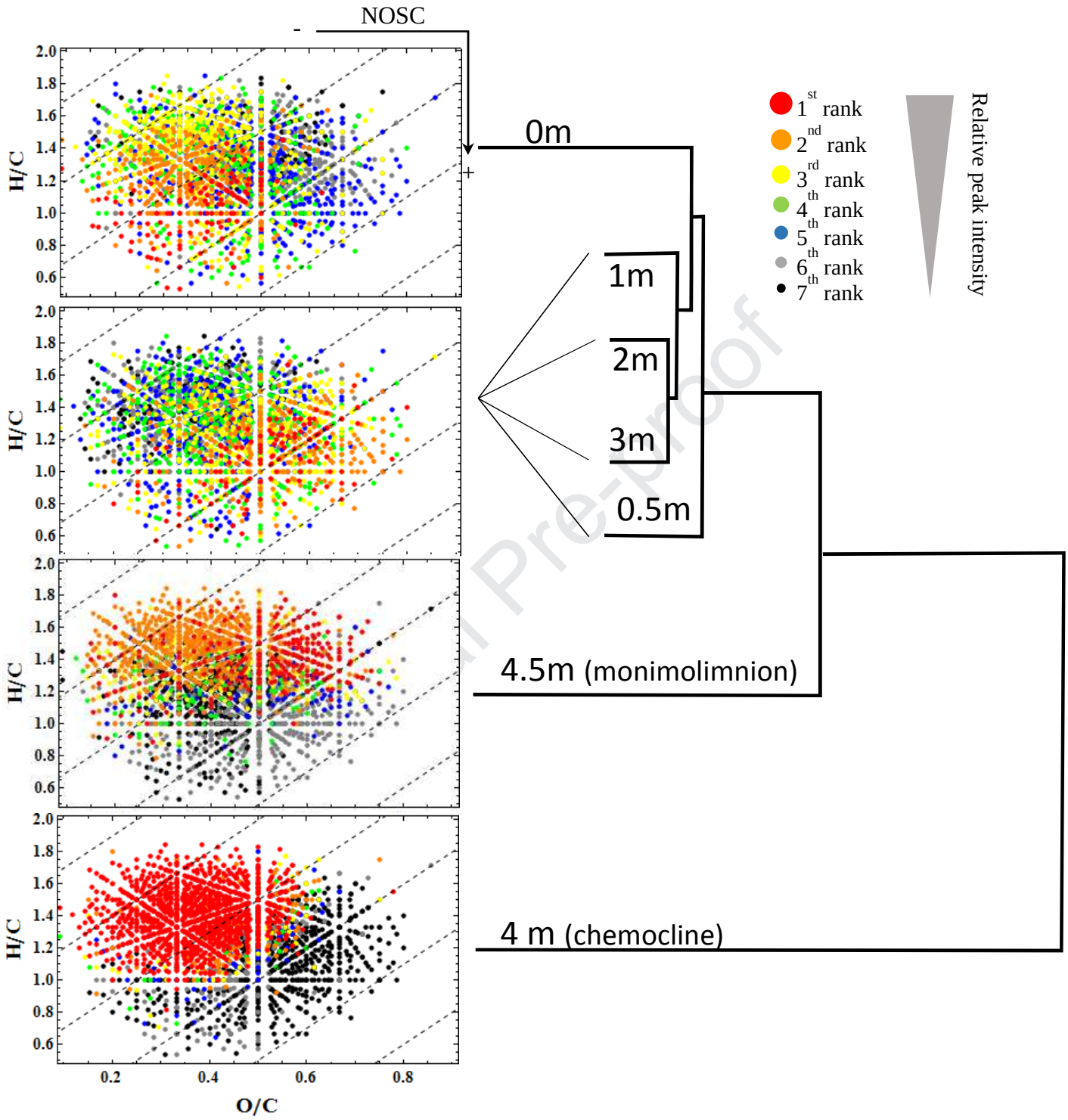

Figure 2. HCA of all SPE-DOM components detected with FT-ICR-MS and van Krevelen diagrams showing the inter sample rankings and molecular composition of SPE-DOM in the water column. Samples at 0, 0.5, 1, 2 and 3 m depth are within the mixolimnion. See appendix SI 3-6 for specific Van Krevelen diagrams of CHO, CHN1S, CHN2O and CHOS molecules

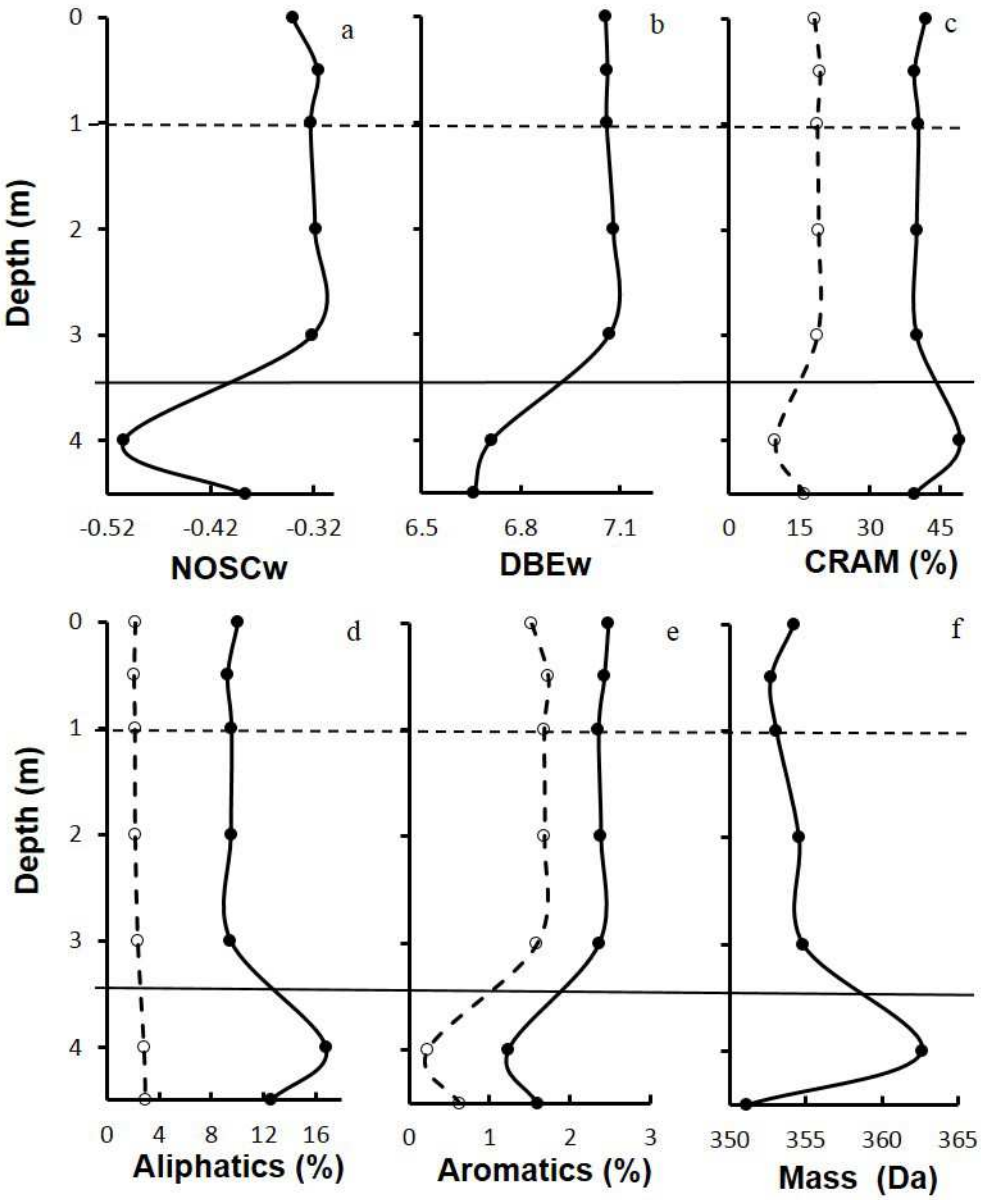

Figure 3. Vertical profiles of two SPE-DOM molecular descriptors (NOSC and DBE) and four molecular classes (CRAM, aliphatic, aromatic and peptides) and molecular size (Mass). All values are weighed averages of peak intensities. Dashed and solid lines in profiles of CRAM, Aliphatic and Aromatic indicate O-rich and O-poor molecules respectively. The two horizontal lines describe the approximate depth of oxycline/thermocline (dashed line) and chemocline (solid line).

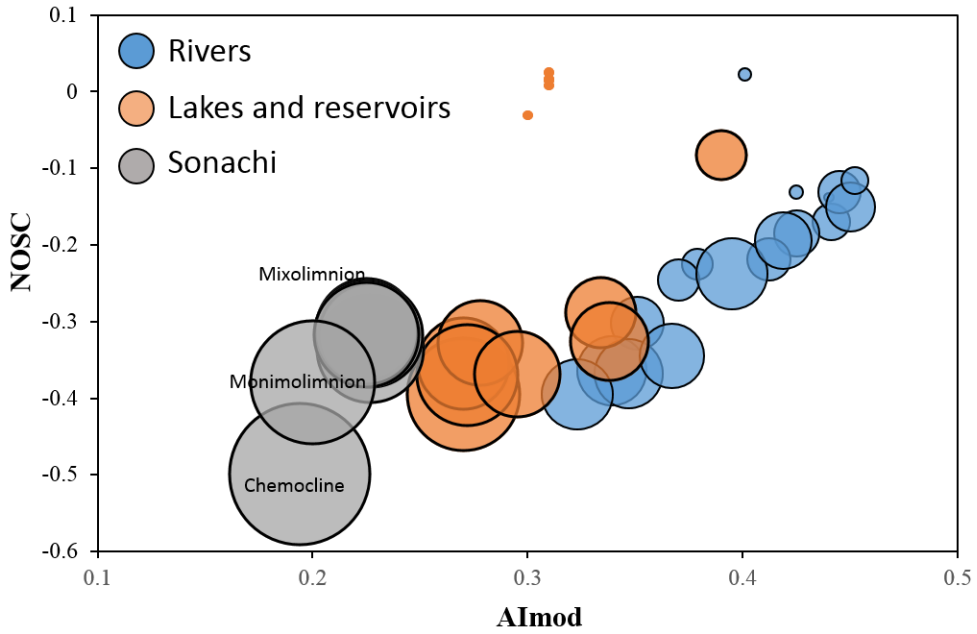

Figure 4. Bubble plot describing the relationship between saturation degree (AImod) and Carbon oxidation state (NOSC) in rivers (blue bubbles) lakes and reservoirs (orange bubbles) and Sonachi (gray bubbles). Bubbles size is proportional to the relative abundance of aliphatic molecules. Literature data are from Kellerman, et al. (2018). Small orange dots are values measured from Rappbode reservoir (Dadi et al., 2017)

Highlights

- First detailed description of DOM in a tropical meromictic saline-alkaline lake.
- High amount of autochthonous DOM was found in water column.
- Solid-phase extracted DOM is microbially derived, photodegraded and aliphatic.
- Changes in DOM quantity and quality were located at the chemocline.